

## REVIEW

[View Article Online](#)  
[View Journal](#) | [View Issue](#)Cite this: *Chem. Sci.*, 2022, 13, 8727

Received 20th June 2022

Accepted 4th July 2022

DOI: 10.1039/d2sc03441g

[rsc.li/chemical-science](https://rsc.li/chemical-science)

## Applications of metal–organic framework-based bioelectrodes

Vidushi Aggarwal,<sup>a</sup> Shipra Solanki<sup>ab</sup> and Bansi D. Malhotra<sup>id</sup>\*<sup>a</sup>

Metal–organic frameworks (MOFs) are an emerging class of porous nanomaterials that have opened new research possibilities. The inherent characteristics of MOFs such as their large surface area, high porosity, tunable pore size, stability, facile synthetic strategies and catalytic nature have made them promising materials for enormous number of applications, including fuel storage, energy conversion, separation, and gas purification. Recently, their high potential as ideal platforms for biomolecule immobilization has been discovered. MOF-enzyme-based materials have attracted the attention of researchers from all fields with the expansion of MOFs development, paving way for the fabrication of bioelectrochemical devices with unique characteristics. MOFs-based bioelectrodes have steadily gained interest, wherein MOFs can be utilized for improved biomolecule immobilization, electrolyte membranes, fuel storage, biocatalysis and biosensing. Likewise, applications of MOFs in point-of-care diagnostics, including self-powered biosensors, are exponentially increasing. This paper reviews the current trends in the fabrication of MOFs-based bioelectrodes with emphasis on their applications in biosensors and biofuel cells.

## 1 Introduction

Molecule-based porous compounds have successfully found utility in diverse areas, including gas adsorption/storage, separation, catalysis, environmental remediation, energy, optoelectronics, and health. Metal–organic frameworks (MOFs), zeolites and covalent organic frameworks (COFs) are the three most common types of 3D porous covalent polymers (PCPs) reported

<sup>a</sup>Nanobioelectronics Laboratory, Department of Biotechnology, Delhi Technological University, Shahbad Daultapur, Delhi 110042, India. E-mail: [bansi.malhotra@gmail.com](mailto:bansi.malhotra@gmail.com)

<sup>b</sup>Department of Applied Chemistry, Delhi Technological University, Shahbad Daultapur, Delhi 110042, India. E-mail: [bansi.malhotra@gmail.com](mailto:bansi.malhotra@gmail.com)



Vidushi Aggarwal has recently obtained her Bachelor of Technology (B. Tech) in Biotechnology from Delhi Technological University (DTU), India. She is a recipient of the IASc-INSA-NASI Summer Research Fellowship 2021 at the Institute of Bioinformatics (IOB), Bengaluru, India. Recently, she was shortlisted for sponsored Idea development in the Tata Steel MaterialNEXT 3.0 challenge for

a research project based on nanomaterials for water remediation. She has been a finalist in the NASA International Space Apps Challenge 2020. Her main areas of interest include metal–organic frameworks, nanomaterials, biosensors and cancer therapeutic targeting. She is highly motivated to pursue a career in translational research with the aim of contributing to patient-centered care and innovative medicine.



Shipra Solanki received her PhD in Chemical Sciences from AcSIR, CSIR-National Physical Laboratory, in 2019. She is presently working as CSIR-RA at the Department of Applied Chemistry, Delhi Technological University, Delhi, on the development of self-powered biosensors for disease detection. She has published more than eleven research articles in international journals and a book

chapter. Her main areas of interest include nanomaterials, thin films, electrochemistry and biosensors.



in the literature. Compared to zeolites, MOFs and COFs can be readily tuned in terms of their pore size, aperture shape and functionality.<sup>1</sup> COFs constitute versatile networks constructed using covalent bonds (B–O, C–C, C–H, C–N, *etc.*) between the organic linkers and MOFs. These can be formed *via* coordinate bonding between metal ions and organic ligands.<sup>2</sup> Both classes of compounds have offered nanoporous materials with high surface areas and diverse pore dimensions, topologies and chemical functionalities. We will only discuss MOFs-based applications in this review.

Generally, d-block transition elements with high coordination numbers such as Zn, Cu, Co and Fe are chosen as metal ions, while multi-dentate organic ligands with a rigid backbone such as benzene-1,4-dicarboxylic acid (BDC), benzene-1,3,5-tricarboxylic acid (BTC), naphthalene-1,4-dicarboxylic acid and 2-ethyl-1H-imidazole are used as linkers. The main attraction of MOFs is their well-defined and tunable pore sizes conferring large internal pore volumes, which serve as a hub for guest molecules like proteins, nucleic acids, and carbohydrates. More recently, the concept of secondary porosity in MOFs has been explored by engineering its surface chemistry in terms of particle size, shape and texture.<sup>3</sup> Another captivating feature of MOFs is their ultrahigh specific surface area (possibly up to 7000 m<sup>2</sup> g<sup>−1</sup>), which is measured using Brunauer–Emmett–Teller (BET) analysis. Their high BET area makes MOFs promising candidates for application in hydrogen storage, carbon capture and drug delivery. Mechanical flexibility is another lucrative property of MOFs, which allows them to be sized and

structured according to specific applications.<sup>4</sup> A myriad of MOFs have been used for applications in gas storage,<sup>5</sup> electrocatalysis,<sup>6</sup> biosensing,<sup>7</sup> drug delivery<sup>8</sup> and environmental remediation.<sup>9</sup>

In this sense, MOFs have emerged as suitable materials in the fabrication of electrodes due to their rigid and malleable structure with redox activity and low cost. They have been extensively explored as anodes, cathodes and electrolyte materials in electrochemical systems. The high porosity and surface area of MOFs-based electrodes are highly favorable for an electrocatalytic role in oxygen reduction reaction (ORR) with great control over structural and chemical properties. Recently, the application of MOFs-based bioelectrodes in electrochemical biosensors and biofuel cells has flourished. Their advantageous properties such as tunable structure, ultrahigh porosity along with stabilizing host–guest interactions adeptly fit the design criteria of bioelectrodes. The characteristic porous framework favors high enzyme loading with improved structural and functional stability. MOFs serve as an ideal microenvironment to protect an enzyme from denaturation and also reduce leaching through hydrophobic interactions and covalent linkages. MOFs pores act as mini-reaction cells, optimizing the mass and charge transfer in biocatalysis. MOFs-based bioelectrodes are suitable for high electrocatalytic current density and low charge resistance as well. Some typical examples include zeolitic imidazolate frameworks (ZIFs),<sup>10</sup> and porous coordination networks (PCNs),<sup>11,12</sup> Fe-based MOFs<sup>13</sup> Mn-based MOFs,<sup>14</sup> Co-based MOFs,<sup>15</sup> and Ni-based MOFs<sup>16</sup> as promising electrode materials in electrochemical biosensors and enzymatic biofuel cells (EBFCs).

In this paper, we discuss the application of MOFs and their derivatives and various components of EBFCs followed by brief applications in biosensors. Fig. 1 shows a summary of the different properties and applications of MOFs. We expect to promote knowledge transfer from the previous studies of MOFs as electrocatalysts, electrolyte membranes, candidates for biomolecule retention, and fuel storage. We present an overview and discuss the recent advances in the development of MOFs in bioelectrocatalytic applications to generate new thoughts.

## 2 Synthesis and modification of MOFs for electrochemical applications

More than 90 000 MOFs have been reported worldwide while around 500 000 more are predicted to be synthesized. Common routes adopted for the synthesis of MOFs include solvothermal, hydrothermal, and solvent-free techniques,<sup>17</sup> as summarized in Fig. 2.<sup>17</sup> The conventional solvothermal synthesis is based on the dissolution of the metal precursor and organic ligand in a suitable solvent such as *N,N*-dimethylformamide (DMF) and ethanol while water is used in case of hydrothermal synthesis. The structure and properties of MOFs are carefully governed by a combination of metal ion, organic ligand, solvent as well as synthesis method. Some of the advantages of the different synthetic methods used in MOF synthesis are summarized in Table 1.



*B. D. Malhotra received his PhD from the University of Delhi, Delhi, in 1980. He has published more than 330 papers in refereed international journals (citations: 25711; index: 85), has filed 11 patents (in India and overseas), and has co-authored a textbook on Nanomaterials for Biosensors: Fundamentals and Applications. He is the recipient of the National*

*Research Development Corporation Award 2005 for the invention of a 'Blood Glucose Biochemical Analyzer' and is a Fellow of the Indian National Science Academy, the National Academy of Sciences, India, and an Academician of the Asia Pacific Academy of Materials (APAM). His current research activities include biosensors, point-of-care diagnostics, nano-biomaterials, biofuel cells, ordered molecular assemblies, conducting polymers, Langmuir–Blodgett films, self-assembled monolayers, advanced functionalized nanosystems, hybrid nanosystems, nano-biotechnology, biomedical engineering, and biomolecular electronics. Dr Malhotra is a former DST-SERB (Govt. of India) Distinguished Fellow and a Chief Scientist, CSIR-National Physical Laboratory(NPL), Delhi, India. Since 1994, he has been exploring functional materials for bio-sensing applications.*



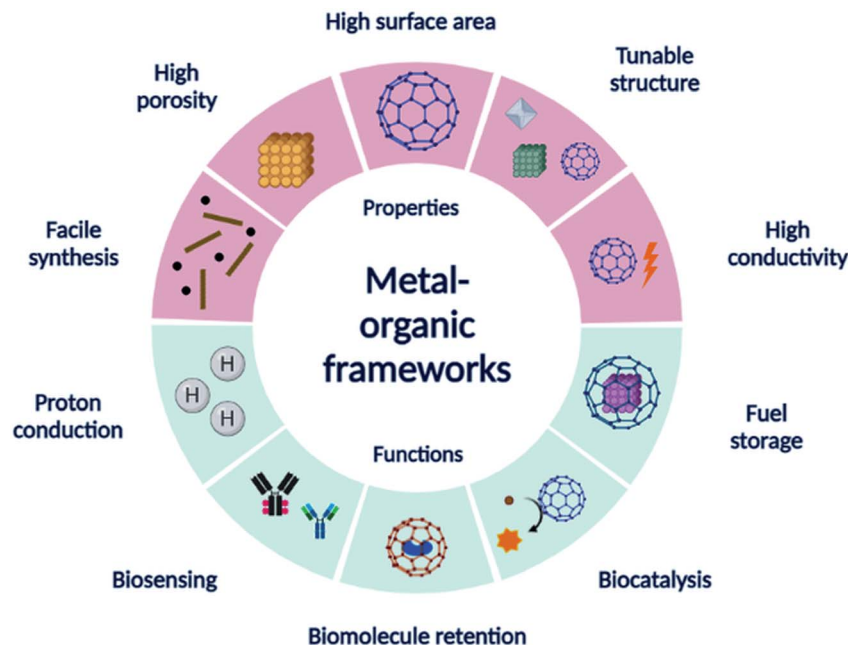


Fig. 1 Various properties and applications of MOFs.

While MOFs have been the front runners in gas storage, separation, and catalysis, applications harnessing their electronic capabilities have been recently realized. Since most MOFs do not have free charge carriers and have low-energy barriers, MOFs were believed to be inherently insulating, limiting their electrochemical applications. Despite having conductivity lower than  $10^{-10} \text{ S cm}^{-1}$ , which makes a material insulating in nature, MOFs can be tailored to achieve superior ionic and protonic conductivity by use of appropriate redox-inactive nodes and short linkers.<sup>18</sup> Many methods, including *in situ* and post synthetic modifications, have been adopted to improve their electrical conductivity, which include composite formation, use of functional linkers, doping,<sup>19</sup> and carbonization. Most methodologies include introducing functionality into MOFs *via* direct synthesis approaches. However, these may not be perhaps suitable sometimes because of challenges like insolubility of the linker, thermal and chemical stability, functional group compatibility, and interference between metal ions and linkers during the assembly of MOFs. To overcome these problems, post-synthetic approaches have been suggested. These can be *via* three modes, including post-synthetic modification (PSM), post-synthetic deprotection (PSD), and post-synthetic exchange (PSE).<sup>20</sup> Doping with nitrogen, sulfur, and phosphorus on MOF precursors is found to increase charge delocalization, catalytic centers, and electron transfer, thereby improving overall ORR performance.<sup>21</sup> Another approach commonly used is the carbonization of MOFs with great scope in electrochemical storage devices.<sup>22</sup> It has the advantage of no additional requirement of primary carbon source as it is fulfilled by the organic ligand. Carbonized MOFs demonstrate remarkable surface area and electrochemical performance with facile synthesis techniques. Different synthetic approaches

adopted to synthesize MOFs for electrochemical applications are summarized in Fig. 3.

Precisely functionalized MOFs can accelerate the electrochemical processes as compared to CNT, graphene, or other nanomaterials based electrodes by also acting as active redox centres.<sup>18</sup> In MOFs, electrical conductivity depends on its metal-cation nature and coordination chemistry while internal ionic conductivity depends on ligand-ion interactions, hydrophilicity, functional groups, and interactions with guest molecules.<sup>23</sup> The nature of counter ions also elicits the electrochemical response of MOFs known as the ion-size effect. As observed in cyclic voltammetry (CV), smaller anions and cations provide stronger response through a series of faradaic reactions.<sup>24</sup> Electrochemical stability and reversibility are other important parameters to be considered in MOF-based systems. Stability is measured as the retained electrochemical response after repeated cycles, whereas reversibility is rapid electron transfer at the interface of electrode and electrolyte, both are crucial for good electrochemical performance. Charge transfer in MOFs can take place through three routes, namely in-plane  $\pi$ -conjugation,<sup>25</sup> through-bond<sup>26</sup> and through-space<sup>27</sup> charge transfer approaches. In-plane  $\pi$ -conjugated MOFs demonstrate high charge mobility and efficient charge delocalization that can be beneficial for many electrochemical applications. On the other hand, the through-bond approach increases electrical conductivity by the participation of delocalized electrons of metal/linker in charge conduction while through-space by  $\pi$ - $\pi$  interaction or electron hopping with guest molecules. These approaches allow better orbital overlapping and thus small band gaps, which results in superior electrical conductivity of MOFs.

Despite all the advantages, pristine MOFs display superior electrochemical properties only when combined with conduct



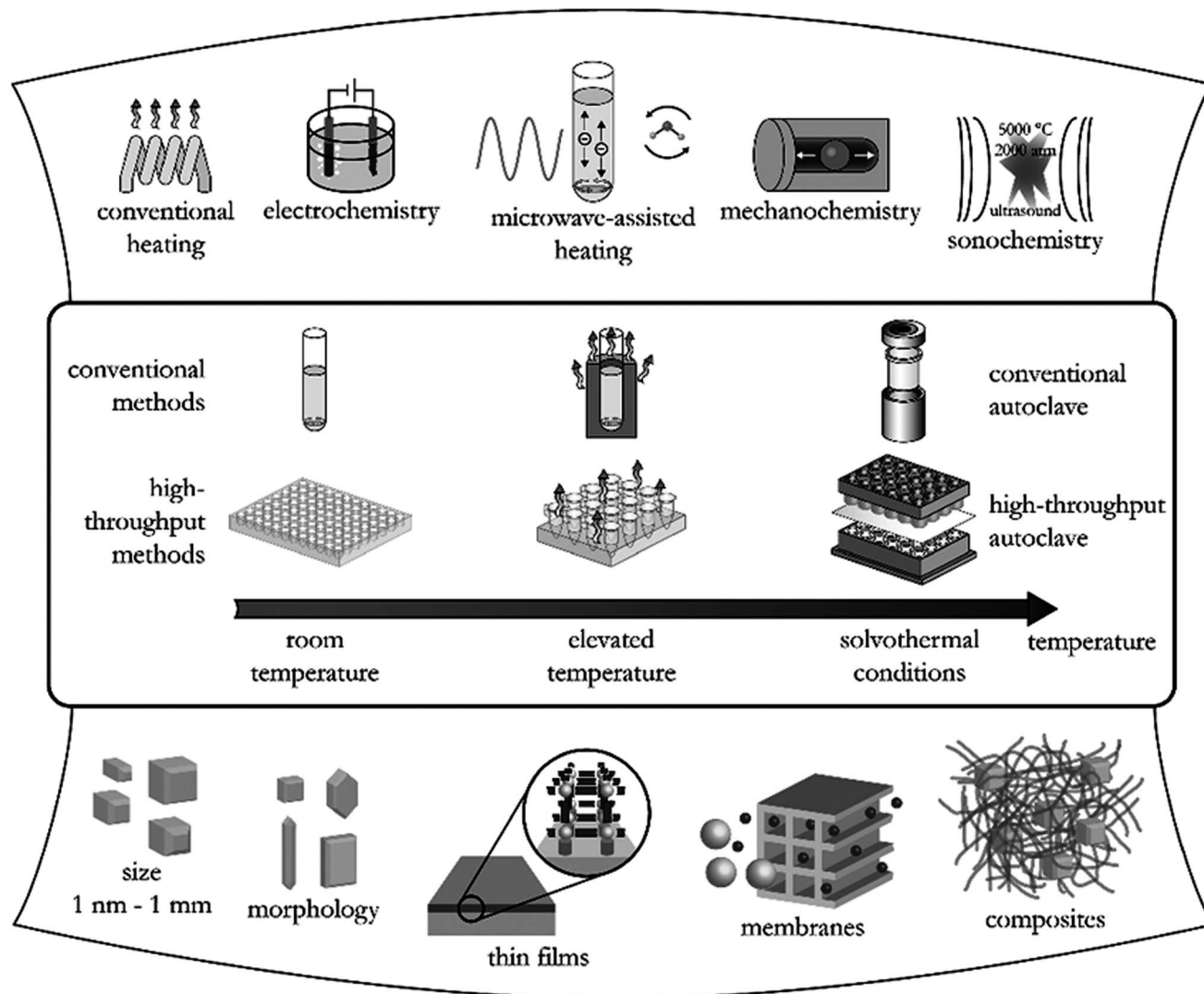


Fig. 2 Different synthetic methods, possible reaction temperatures, and final reaction products in MOFs synthesis.<sup>17</sup>

materials. Conducting MOFs is an upcoming field of research with high expectations in electrochemical applications. While there are limited studies on the commercial potential of conducting MOFs, promising outcomes of MOFs as electrochemical sensors and energy storage are being extensively explored.

### 3 MOFs and biomolecule retention

Immobilization of biomolecules is an important aspect in the fabrication of ideal bioelectrodes to minimize leaching and functional stability. The ultrahigh porosity and surface area of MOFs have been exploited for biomolecule retention. A wide range of biomolecules such as proteins (enzymes, antibodies), carbohydrates, and nucleic acids can be accommodated in MOFs pores as well as linked to their outer surface.<sup>28</sup> Various MOFs are immobilized on the surface of bioelectrodes through covalent, electrostatic, hydrophobic, and van der Waals forces.<sup>29</sup> It results in increased loading of biocatalysts due to increased

surface area. The four common approaches used for the retention of biomolecules in MOFs are adsorption, bio-conjugation, encapsulation, and diffusion, as discussed below.

#### 3.1 Adsorption

Surface attachment of biomolecules to the MOFs can be accomplished in two ways – through surface bonding and by general adsorption. It is a common method for preparing biomolecule-MOFs composites. Biomolecules are anchored to the MOFs surface through weak interactions with no requirement of specific functional groups. Recently, Ma *et al.* used a series of ZIFs as adsorption matrices for immobilization of electrocatalysts, namely glucose dehydrogenase (GDH) and methylene green (MG) in glucose biosensor.<sup>30</sup> ZIF-70, with the largest pore size, was the most efficient matrix for co-immobilization amongst ZIF-7, ZIF-8, ZIF-67, and ZIF-68, in the fabricated bioelectrode as shown in Fig. 4(a). ZIF-70 demonstrated outstanding adsorption capacities towards electrocatalysts and therefore higher sensitivity and selectivity





**Table 1** Overview of the synthetic methods of MOFs along with their features, temperature-duration and advantages

S. no.	Synthetic methods	Features	Temperature-duration	Advantages
1	Solvothermal (hydrothermal)	Solvents such as water, DMF used	At 353–453 K for 2–3 days	<ul style="list-style-type: none"> <li>• High yield of MOF</li> <li>• High surface area and porosity of MOF</li> <li>• Highly crystalline MOF</li> </ul>
2	Non-solvothermal	Under the boiling point of solvent	At 298 K for several days to months	<ul style="list-style-type: none"> <li>• Carried out at room temperature or simple heating</li> <li>• Simple equipment required</li> </ul>
3	Electrochemical	Through anodic dissolution or cathodic deposition	At 273–303 K for 10–30 min	<ul style="list-style-type: none"> <li>• Suitable for synthesis of large quantity of MOF</li> <li>• No formation or separation of anions required</li> </ul>
4	Mechanochemical	Chemical transformation through milling or grinding	At 298 K for 30 min <sup>−2</sup> h	<ul style="list-style-type: none"> <li>• No washing or activation required</li> <li>• Suitable for metal precursor with low solubility</li> </ul>
5	Microfluidics	Reaction in microfluidic channel	At 323–423 K for few minutes	<ul style="list-style-type: none"> <li>• Fast crystallization rate</li> <li>• Great control over morphology of MOF crystal</li> </ul>
6	Microwave-assisted	Interaction between reactants and radiation	At 303–373 K for 4 min <sup>−4</sup> h	<ul style="list-style-type: none"> <li>• Good efficiency in short duration</li> <li>• Great control over reaction parameters and morphology of MOF crystals</li> </ul>
7	Ionothermal	Ionic liquids used as solvent and template	At 333–373 K for 6 h	<ul style="list-style-type: none"> <li>• Environmentally-friendly method</li> <li>• Great control over morphology of MOF crystals</li> </ul>
8	Sonochemical	Ultrasonic waves used for acoustic cavitation effect	At 272–313 K for 30–180 min	<ul style="list-style-type: none"> <li>• Fast crystallization rate</li> <li>• Suitable for small particle size</li> </ul>
9	Spray drying	Atomization of MOF precursor solution using spray drier	At 423–453 K for 5–10 min	<ul style="list-style-type: none"> <li>• Fast and simple technique</li> <li>• Suitable for multi-metallic MOFs</li> </ul>
10	Flow chemistry	Continuous MOF synthesis in tube reactors	At 353 K for 5–10 min	<ul style="list-style-type: none"> <li>• Low material and energy consumption</li> <li>• Ease in down streaming</li> </ul>

towards glucose with a linear range of 0.1–2 mM. The approach was highly beneficial due to various advantages offered by highly porous ZIF-70, such as better adsorption capability and chemical stability due to interaction with functional groups. Interestingly, MOFs have also been used in the development of biosensors for SARS-COV-2 detection.<sup>31</sup> MOF surface could provide an efficient adsorption platform for fluorophore-labeled probes through electrostatic interactions, hydrogen bonding, and  $\pi$ - $\pi$  stacking. Moreover, there is possibility of increased recovery of fluorescence due to the weak affinity of hybridized DNA towards MOFs. MOFs as adsorption and fluorescence quenching platform could therefore increase the sensitivity and rapidity of detection in SARS-COV-2. The adsorption technique is quicker and easier as compared to other techniques with no strict requirement on MOF's pore size. This technique also allows reaction parameters to exceed the denaturing limits of biomolecules as it could be adsorbed after MOFs synthesis. Adsorption also enables better recovery and recyclability of biomolecules in repeated cycles. However, due to the weak

protection effect of MOFs, exposed biomolecules could easily detach from the MOFs surface and are prone to leaching. Therefore, there is a growing need for alternative immobilization methods using porous nanomaterials.

### 3.2 Conjugation with linker

Bioconjugation refers to either covalent linkage or electrostatic force of attraction to anchor biomolecules on the MOFs surface. The bio-functionalized MOFs synthesised through this approach are advantageous for simplistic electrochemical bio-sensing and signal amplification. Biomolecules covalently attached with MOFs functional groups are highly stable and exhibit improved catalytic activity. A porphyrin-functionalized MOFs bioconjugated with streptavidin (SA) named as FeTCPP@MOF-SA using HKUST-1(Cu) as shown in Fig. 4(b) was fabricated for DNA sensing.<sup>32</sup> The setup enabled highly sensitive and specific recognition through the allosteric switch of hairpin DNA. The LOD of 0.48 fM was recorded with the linear range of 10 fM to 10 nM. HKUST-1(Cu) supported a label-free detection



## Synthesis of Electrochemically active MOFs

## Direct synthesis approaches

- MOFs with redox active metal centres
- MOFs with redox active ligands
- Doped MOFs
- MOF composites with metals, metal oxides, CNTs, graphene and conducting polymers

## Post synthetic approaches

- Modification of organic ligands via chemical reactions
- Replacement of ligands in pre-assembled MOFs
- Carbonisation of MOFs

Fig. 3 Different approaches to synthesize electrochemically active MOFs.

approach by working as a signal probe for mediating recognition between SA and aptamer. Bioconjugated MOFs present new avenues for mimetic catalysis as a promising signal

transduction platform. In another work by Kumar *et al.*, MOF-5 was bioconjugated with anti-bovine serum albumin (anti-BSA) for electroluminescence biosensing.<sup>33</sup> The pendent (side)

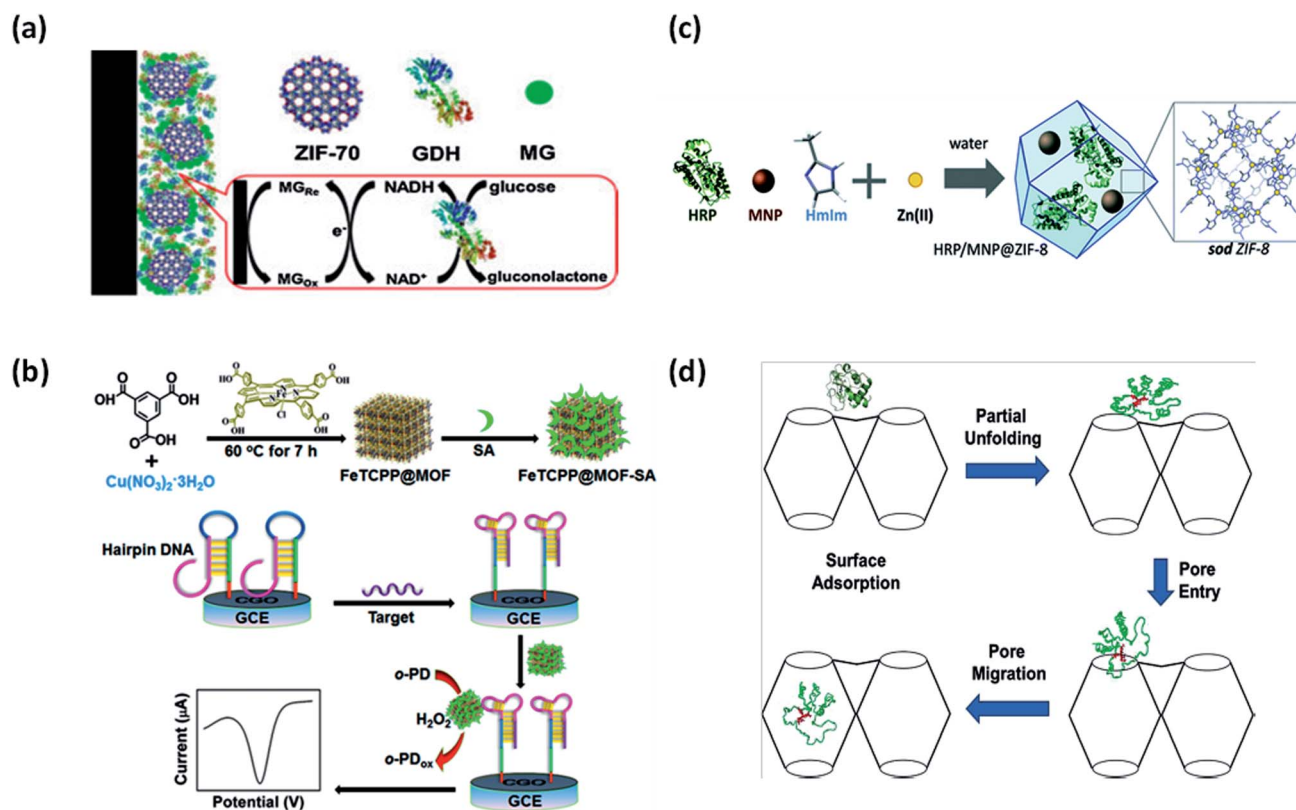


Fig. 4 Different immobilization strategies using MOFs. (a) Adsorption of glucose dehydrogenase (GDH) at ZIF-70 surface.<sup>30</sup> (b) Bioconjugation of FeTCPP@MOF with streptavidin (SA).<sup>32</sup> (c) Encapsulation of horseradish peroxidase (HRP) and magnetic nanoparticles (NPs) in ZIF-8.<sup>34</sup> (d) Diffusion of Cyt c into the cavities of Tb-mesoMOF.<sup>35</sup>



group on MOF-5 surface was activated through simple organic reactions followed by covalent protein conjugation with anti-BSA. The pendent group of the organic linker was activated using 1-ethyl-3-(3-dimethylaminopropyl)carbodiimide (EDC). Despite strong bioconjugation of anti-BSA on MOF-5, no loss of enantioselectivity was observed. This study further encouraged the application of MOFs in molecular sensing and immuno-histochemistry assays. One major advantage of using this approach is strong interaction between biomolecule and MOFs, which guarantees structural stability. The formation of robust peptide bonds between amino group of enzyme and carboxylate group of MOFs is highly feasible in bioconjugation. Moreover, higher recyclability of biomolecules is assured since there are minimal chances of leaching. However, in this particular approach, the biomolecule linked to the surface is susceptible to denaturation under harsh conditions, which can be overcome by encapsulation, as discussed in the next section.

### 3.3 Encapsulation

Encapsulation involves capturing the biomolecule within MOFs, which can be *in situ* or *ex situ*. The *in situ* encapsulation has emerged as a powerful tool wherein MOFs grow around biomolecules leading to high loading efficiency and negligible leaching. Encapsulation, being a rapid and low-cost approach, is likely to accelerate the application of important industrial biomolecules in the commercial sector. However, the *in situ* strategy is limited to only operation under mild conditions in aqueous solutions due to the risk of denaturation of biomolecules, greatly restricting the diversity of MOFs. ZIFs can be adopted as suitable nanomaterials for biomolecule encapsulation. Recently, magnetically and catalytically active ZIFs have been proposed as recyclable MOF-based biocatalysts. Ricco *et al.* reported a one-pot synthesis method for dual encapsulation of horseradish peroxidase (HRP) and magnetic NPs in ZIF-8, as shown in Fig. 4(c).<sup>34</sup> A five-fold increase in HRP activity was observed along with improved reusability and specific activity of the enzyme. Encapsulation offers various advantages over other immobilization techniques with respect to stability and prevents the leaching of biomolecules from the host matrix. Additional benefits of size selectivity and substrate specificity can be achieved due to the specific pore size of MOF, which is not possible in surface immobilized biomolecules. MOF surface acts as a protective shell against competitive inhibitors and denaturation agents. Moreover, it physically separates biomolecules, thereby preventing aggregation. However, a major drawback of encapsulation are the inability to accommodate large biomolecules, hindrance in mass transfer efficiency, and accessibility to the biomolecule. Efforts should be made to study the underlying mechanisms and host-guest interactions to develop standard procedures for MOF encapsulation to remediate these limiting issues.

### 3.4 Diffusion

Diffusion is defined as the infiltration of biomolecules within the MOF pores. This technique is especially useful for the immobilization of large biomolecules such as proteins inside

MOFs with relatively small pores. For example, cytochrome c (Cyt c) has been successfully diffused through partial folding within Tb-mesoMOF, as shown in Fig. 4(d).<sup>35</sup> An interesting observation was made regarding the translocation of enzymes through unique conformational changes in enzyme structure at the MOF surface during immobilization. It mimics the activity of proteins undergoing conformational changes during translocation in organelles with narrow pores. This strategy can further open new avenues for MOFs in protein translocation research. Nevertheless, this approach is greatly limited due to concerns over the slow rate of diffusion and enzyme leaching. Unfortunately, limited biomolecules could be immobilized in MOFs through the diffusion process. Therefore, a growing need for better alternatives to overcome these limitations is felt.

All the approaches mentioned above provide better stability to biomolecules. MOFs serve as ideal hosts for biological guests attracting applications in drug delivery, biosensing, bioimaging, bioremediation, genetic manipulation, and preservation of biological specimens.<sup>36–38</sup> With promising applications in biomolecule detection, immunoassays, and tumour detection, various researches focus on achieving technical excellence through size, cost, and materials. Fine tuning of structure and porosity of MOFs for specific applications is also a challenging task. Since high outcomes are anticipated in this field of research, a deeper understanding of internal interactions and mechanisms should be explored. Some bottlenecks such as stability in water and mass transfer limitations also hinder the industrial production of MOFs. Therefore, efforts should be directed to replicate the results from lab to pilot scale.

## 4 MOF-based bioelectrodes for biosensors

Electrochemical biosensors utilize working electrodes with biological recognition elements (BRE) attached for their function. Bioelectrodes act as an interface between biological and electrochemical phenomena, which ultimately determines the overall performance of the biosensor.<sup>39</sup> With the paradigm shift towards point-of-care diagnostics, there is a growing need to achieve exceptional structural and functional stability, biocatalysis, sensitivity, and specificity in bioelectrodes through the use of superior nanomaterials.<sup>8,40</sup> MOFs can be explored as host matrix, biocatalyst, and BRE in bioelectrodes for biosensors as discussed. Table 2 provides a summary of recently reported MOFs-based bioelectrodes in electrochemical biosensors.

### 4.1 MOFs as host matrix

Enzyme-based biosensing devices require optimum thermal, chemical, and mechanical environment for proper action and tend to denature under harsh conditions. Therefore, there is a need to provide a suitable working environment for enzymes for their optimum functioning. MOFs have emerged as suitable host matrices for enzyme immobilization due to their remarkable surface area, crystalline nature, porous framework, and high flexibility. MOFs with a large free volume easily



Table 2 MOFs-based bioelectrodes used in electrochemical biosensors<sup>a</sup>

S. no.	MOF	Biological recognition element	Target analyte	LOD	Linear range	Reference
1	Co-MOF, ZIF-67	Cobalt oxide hollow nanododecahedra (Co <sub>3</sub> O <sub>4</sub> -HND)	Glucose	0.58 $\mu\text{M}$	2.0 $\mu\text{M}$ to 6.06 mM	88
2	Cr-MOF (MIL-53-CrIII)	—	H <sub>2</sub> O <sub>2</sub>	3.52 $\mu\text{M}$	25 to 500 $\mu\text{M}$	89
3	Cu-MOF	Hemin	H <sub>2</sub> O <sub>2</sub>	0.14 $\mu\text{M}$	10 to 24 400 $\mu\text{M}$	90
4	Cu-MOF	GOx	Glucose	14.77 $\mu\text{M}$	44.9 $\mu\text{M}$ to 4.0 mM	91
5	Cu-MOF	Tyrosinase	BPA	13 nmol l <sup>-1</sup>	5.0 $\times 10^{-8}$ to 3.0 $\times 10^{-6}$ mol l <sup>-1</sup>	92
6	Cu-MOF	—	miRNA	0.35 fM	1.0 fM to 10 nM	93
7	Fe-MIL-88-NH <sub>2</sub>	Hemin	ADRB1 gene	0.21 fM	1 fM to 10 nM	46
8	Fe-MOF	Pb <sup>2+</sup> -specific DNzyme	Pb <sup>2+</sup>	2 pM	0.005 to 1000 nmol L <sup>-1</sup>	94
9	Ni-MOF	—	Urea	3 $\mu\text{M}$	0.01 to 1.12 mM	95
10	Ni-MOF	—	Glucose	4.6 $\mu\text{M}$	20 $\mu\text{M}$ to 4.4 mM	96
11	Pb-BDC-NH <sub>2</sub>	anti-CEA	Carcinoembryonic antigen (CEA)	0.03 pg mL <sup>-1</sup>	0.3 pg mL <sup>-1</sup> to 3 ng mL <sup>-1</sup>	97
12	Pb-BDC-NH <sub>2</sub> and Cd-BDC-NH <sub>2</sub>	anti-AFP	Alpha-fetoprotein (AFP)	0.1 pg mL <sup>-1</sup>	0.3 pg mL <sup>-1</sup> to 3 ng mL <sup>-1</sup>	97
13	PCN-333(Al)	Microperoxidase-11 (MP-11)	H <sub>2</sub> O <sub>2</sub>	0.127 $\mu\text{M}$	0.387 $\mu\text{M}$ to 1.725 mM	11
14	Y-1, 4-NDC-MOF	AgNPs	H <sub>2</sub> O <sub>2</sub>	0.18 $\mu\text{M}$	4 to 11 000 $\mu\text{M}$	98
15	Y-1, 4-NDC-MOF	CuNPs	H <sub>2</sub> O <sub>2</sub>	0.43 $\mu\text{M}$	4 to 8500 $\mu\text{M}$	98
16	ZIF-67	—	Glucose	0.99 $\mu\text{M}$	48 $\mu\text{M}$ to 1 mM	99
17	ZIF-67	—	Glucose	0.66 $\mu\text{M}$	2 to 1000 $\mu\text{M}$	100
18	ZIF-8	HRP	H <sub>2</sub> O <sub>2</sub>	0–800 $\mu\text{M}$	1 $\mu\text{M}$	101
19	ZIF-8	LAC and GOx	Glucose	5.347 $\mu\text{M}$	1 to 10 mM	42
20	ZIF-8	BPA	LAC	5.347 $\mu\text{M}$	1 to 20 mM	41

<sup>a</sup> GDH – glucose dehydrogenase, GOx – glucose oxidase, HRP – horseradish peroxidase, ADH – alcohol dehydrogenase, LAC – laccase, BPA – bisphenol A.

accommodate large as well as small enzymes with great control over surface topology. The enzymes adsorbed or entrapped inside MOFs have increased stability and display great tolerance to dynamic pH changes.

Li *et al.* constructed a ZIF-8@LAC (LAC = laccase) based bioelectrode (cathode as well as anode) through encapsulation and surface immobilization techniques for the detection of bisphenol A (BPA).<sup>41</sup> ZIF-8 was combined with bacterial cellulose (BC)/carboxylated multi-walled carbon nanotubes (c-MWCNTs) to provide flexibility. ZIF-8@LAC showed improved biocatalysis, structural stability, and enzyme recyclability. No hindrance in the diffusion process of substrate and product through ZIF-8 was encountered upon loading of LAC. The ZIF-based bioelectrode exhibited LOD of 5.347  $\mu\text{M}$  and a maximum power density of 3.68 W m<sup>-3</sup>. It was successful in removing 98% of BPA within 6 h. In a similar work by the same group, they proposed an EBFC-based self-powered biosensor using ZIF-8 as the host matrix, as shown in Fig. 5(a).<sup>42</sup> They adopted *in situ* growth of ZIF-8 encapsulated with glucose oxidase (GOx) and LAC on cellulose acetate (CA) membrane, followed by MWCNTs and AuNPs absorption. CA/ZIF-8@GOx/MWCNTs/Au was used as bioanode and CA/ZIF-8@LAC/MWCNTs/Au as biocathode in a dual chamber biosensor to monitor glucose levels with LOD of 5.347  $\mu\text{M}$ . The electrodes showed large surface area, porosity, flexibility, and thermal stability due to the use of ZIF-8. The study presents promising

results as a non-invasive glucose biosensor with continuous detection and structural stability of up to 15 h.

MOFs can be utilized to obtain increased recovery and reusability of enzymes for long term usage. MOFs provide a biocompatible microenvironment for enzymatic biosensing of a wide range of analytes. Despite major advantages, leaching out of toxic metal ions poses a great risk to the safe application of MOF-based bioelectrodes. Therefore, there is a great demand for biocompatible MOFs with synergistic effects of both MOFs and enzymes. The biocompatibility of MOFs is determined by factors such as the nature of metal ions and organic linkers along with some physical parameters. Several metals such as Zr and Ti are non-toxic to humans and are suitable for the synthesis of biocompatible MOFs. Likewise, many organic ligands naturally present in the human body, such as aspartate and adenine, could be explored as linkers. Physical properties of MOFs, including shape, size, and charge, also influence their biocompatibility. Moreover, the water stability and biodegradability of MOFs are of utmost importance for ensuring their biocompatibility. On the biomedical front, biocompatible MOFs have the potential to augment drug delivery and translational research as smart nanocarrier systems. The intelligent application of MOFs as an ideal host matrix is expected to open new avenues for the synthesis of robust bioelectrode for biosensors.





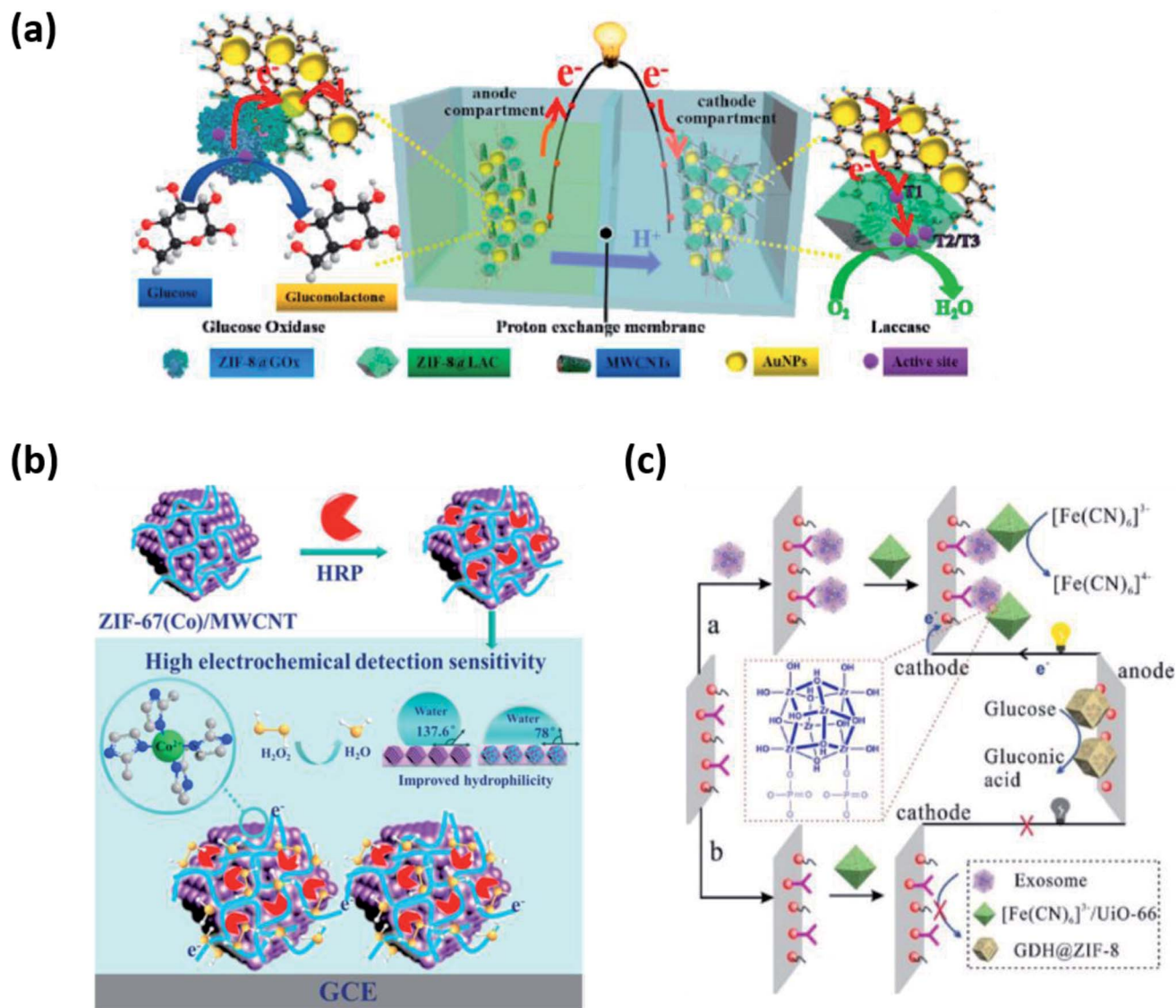


Fig. 5 Applications of MOFs in biosensors (a) ZIF-8 as a host matrix for GOx.<sup>42</sup> (b) PCN-333(Fe) as a synergistic biocatalyst.<sup>44</sup> (c) ZIF-8 as a biological recognition element for exosome detection.<sup>45</sup>

## 4.2 MOFs as electrocatalysts

MOFs not only serve as ideal host matrices but also contribute to synergistic biocatalysis along with enzymes. Several MOFs such as ZIF-8, ZIF-70, and MIL-100(Fe) have been explored to act as catalysts and facilitate electron transfer without compromising the enzyme activity. They help establish electrical communication between the redox enzymes and the bioelectrodes, thereby promoting biocatalysis at low over potentials and high anodic current densities. As an excellent example, a water stable iron-based MOF known as PCN-333(Fe) was employed in the electrochemical biosensing of H<sub>2</sub>O<sub>2</sub>.<sup>43</sup> It demonstrated an LOD of 0.09  $\mu$ M in the detection range of 0.5  $\mu$ M to 1.5 mM. PCN-333(Fe) immobilized with HRP showed synergistic catalytic properties of both MOF and enzyme. PCN-333(Fe) proved to be advantageous in many aspects (i) the size similarity of PCN-333(Fe) and HRP ensured highly effective

enzyme loading (ii) strong interactions prevented conformational changes of HRP and eliminated the risk of aggregation and leaching (iii) ultrahigh porosity and surface area of PCN-333(Fe) easily accommodated the enzyme without restricting its activity and (iv) most importantly, the presence of Fe<sup>3+</sup> ions in PCN-333(Fe) with intrinsic peroxidase-like activity acted as biocatalyst further improving the sensitivity of electrochemical biosensing. It was observed that PCN-333(Fe) not only ensured more effective shuttling of electrons between the electrode and HRP redox centers but also increased the collision frequency between the analyte and enzyme, thereby contributing to improved biocatalysis. Moreover, the HRP@PCN-333(Fe) modified electrode functioned well in harsh environments (extreme temperature and pH), showing improved operational stability. In another example, ZIF-67 immobilized with HRP was used to increase the sensitivity of electrochemical biosensing of H<sub>2</sub>O<sub>2</sub>, as shown in Fig. 5(b).<sup>44</sup> The MOF-enzyme system

witnessed a 1.3-fold increase in sensitivity recorded as  $315 \mu\text{A mM}^{-1} \text{cm}^{-2}$  with a greater affinity towards  $\text{H}_2\text{O}_2$ . The LOD was recorded as  $0.09 \mu\text{M}$  in the linear range of  $0.5 \mu\text{M}$  to  $1.5 \text{ mM}$ . The researchers have emphasized the synergistic biocatalysis of MOF and enzyme, rendering superior performance to electrochemical biosensors.

Hence, the role of MOFs is quite evident in improving the catalytic efficiency of enzymes and as a result, the sensitivity of electrochemical biosensors. MOFs not only confer structural benefits but also the presence of a metal center fastens the rate of electron transfer further increasing the biocatalytic efficiency of bioelectrodes. The positive impact of MOFs on electrochemical biocatalysis is commendable and holds a great future for advancements in biosensing technologies. Therefore, MOF-based bioelectrodes are gaining increased interest for feasible applications in miniaturized and highly stable biosensors.

### 4.3 MOFs enhancing the sensitivity and selectivity of bioelectrodes

In addition to improving the stability and sensitivity of biosensors, MOFs such as ZIF-8, HKUST-1, Cu-MOF, and Ru-MOF have been reported to function as BRE for capturing and sensing diverse biomolecules such as DNA, RNA along with cancer biomarkers such as exosomes and microRNAs (miRNAs). MOFs are commonly used as a sensing unit to amplify electrochemical signals exploiting their biomimetic catalytic feature. It has been observed that MOFs simultaneously provide enhanced sensitivity and selectivity through strong covalent bonding, electrostatic attractions, hydrogen bonding, and hydrophobic interactions between the analyte and metal node/linker.

Recently, a self-powered biosensor based on dual MOFs bioelectrodes for the detection of exosomes, a cancer biomarker, has been reported. A GDH@ZIF-8 modified anode and a  $[\text{Fe}(\text{CN})_6]^{3-}/\text{UiO}-66$  modified cathode were fabricated in order to achieve more stable and sensitive exosome biosensing, as shown in Fig. 5(c).<sup>45</sup> It was observed that ZIF-8 provided better catalytic efficiency and stability to GDH. On the other hand,  $[\text{Fe}(\text{CN})_6]^{3-}/\text{UiO}-66$  served as nano-enrichment carriers by accepting electrons from the anodic oxidation, generating electrical power. Dual MOF-based bioelectrodes enabled additional sensitivity through the formation of Zr–O–P bonds between the metal node of UiO-66 and phosphate groups of an exosome phospholipid bilayer. The LOD was noted to be 300 particles per mL. The aforementioned dual MOFs bioelectrodes based SPB was also successful in identifying exosomes from different cell lines conferring specificity. Further improvement in the anti-interference ability of the biosensor by use of nanomaterials holds great promise in the early diagnosis and treatment of cancer.<sup>9</sup> Yuan *et al.* modified glassy carbon electrode attached with Fe-MIL-88-NH<sub>2</sub> probe loaded with Cu(II) ions, hemin, and PtNP.<sup>46</sup> The fabricated bioelectrode Pt/Hemin@Fe-MIL-88-NH<sub>2</sub>/Cu<sup>2+</sup> not only assisted in the synergistic electrocatalytic oxidation of  $\text{H}_2\text{O}_2$  but also improved binding affinity towards the substrate. The LOD was noted to be  $0.21 \text{ fM}$  in the range of  $1 \text{ fM}$  to  $10 \text{ nM}$ . The technique proved promising from a clinical point of view, with no longer needing to label or

pre-amplify samples. However, the fabrication process is quite long. There is thus a need to achieve a consistent methodology for better stability of biosensors.

MOF-based biosensors are commercially promising in terms of rapid detection and facile synthesis and present an exciting method for real time and point-of-care diagnostics. Their tunable properties, wide range of working conditions (extreme temperature and pH), and low cost of fabrication make them suitable for scale-up in the biomedical industry. However, some limitations in the area of binding kinetics, electric communication between enzyme and electrode, multiplexed analyses, and MOF-coupled transducers remain to be addressed. There are limited studies regarding biocompatibility, toxicity, stability in water, and false-positive results are some bottlenecks limiting the mass production of MOF-based bioelectrodes for biosensors. Nevertheless, efforts should be made to circumvent these issues for improved performance of MOF-based bioelectrodes in biosensors.

## 5 MOF-based bioelectrodes for biofuel cells

Fuel cells are regarded as one of the best green renewable technologies with the ability to harvest electrical energy from the chemical energy of biological processes.<sup>47,48</sup> Since its invention in 1964 by Yahiro *et al.*, EBFCs have witnessed structural and functional advancements for the past six decades.<sup>49</sup> Nanomaterials such as carbon nanotubes and metal NPs are the fore-runners and hence are the ideal choice for various uses in EBFCs and biosensors. More recently, MOFs have found versatile roles in EBFCs in and as bioelectrodes, electrocatalysts, electrolyte membrane, biomolecule retention, and fuel storage. Table 3 provides a summary of recently reported MOFs-based bioelectrodes in biofuel cells.

### 5.1 MOFs as electrocatalysts

In the past decade, enzyme@MOFs combination has been thoroughly explored as promising electrobiocatalysts. Lower stability, reusability, and recovery of enzymes are limitations in mass production. Enzymes such as lipase,<sup>12</sup> hydrolase,<sup>50</sup> catalase,<sup>20</sup> and GOx,<sup>51</sup> when immobilized on MOF surface, offer various advantages to overcome these limitations. The high surface area of MOFs is perfect for high enzyme loading, and its porous structure supports enzyme ingress and diffusion of substrates and products. However, poor conductivity and instability during solvent extraction in MOFs are some functional limitations. With improved electrocatalytic activity and stability, functionalized MOFs offer dual functionality in fabrication as well as encapsulation of NPs.

In an effort to obtain superior properties of MOFs in MOF-derived NPs, several researchers have used MOF templates as precursors for the synthesis of transition metal/metal oxide carbon and carbon NPs such as M–N–C, M–MO<sub>x</sub>–N–C, N-doped-C and NP-C as electrocatalysts.<sup>22,52,53</sup> ZIF-67, a Co-based MOF was reported as a precursor for the fabrication of doped carbon nanotubes of hollow frameworks (NCNTF-700).<sup>54</sup> ZIF-67 has



Table 3 MOF-based bioelectrodes in biofuel cells<sup>a</sup>

S. no.	MOF	Function of MOF used	Fuel (oxidised)	Power density/current density	Reference
1	ZIF-8	Nanocarriers	Glucose	23 $\mu\text{W cm}^{-2}$	82
2	Al-PCP	Immobilization of GOx	Glucose	0.548 $\text{mW cm}^{-2}$	102
3	IRMOF-8	Bioanode catalyst	Alcohol	0.25 $\pm$ 0.03 $\text{mA cm}^{-2}$ (current density)	103
4	MAF-7	Biocatalyst	Glucose	119 $\mu\text{W cm}^{-2}$	104
5	Co-MOF, ZIF-67	Electrocatalyst	Glucose	0.3 $\text{mA cm}^{-2}$ (current density)	88
6	MOF derived <i>meso</i> -CuCo <sub>2</sub> O <sub>4</sub> microspheres	Template precursor	Glucose	0.33 $\text{mW cm}^{-2}$	105
7	ZIF-8	Electrocatalyst	Oxygen	—	106
8	MIL-100(Fe)	Immobilization matrix	2,2'-Azino-bis(3-ethylbenzothiazoline-6-sulfonic acid) (ABTS)	—	107
9	Cu-MOF	Electrocatalysts	H <sub>2</sub> O <sub>2</sub>	—	108

<sup>a</sup> GDH – glucose dehydrogenase, GOx – glucose oxidase, HRP – horseradish peroxidase, ADH – alcohol dehydrogenase, ABTS – 2,2'-azino-bis(3-ethylbenzothiazoline-6-sulfonic acid).

been found to provide structural advantage over traditional Pt/C electrocatalysts with improvement in ORR and OER. It exhibited a current density of 10  $\text{mA cm}^{-2}$  at 1.60 V. The bi-functional electrocatalysts exhibited remarkable stability and functionality. It is also worth noting that pyrolysis temperature was indirectly proportional to ORR activity of NCNTF-700, with the best performance at low temperatures. Similarly, many researchers have harnessed the structural advantage of MOFs to produce transition metal/metal oxide based nanocarbon electrocatalysts.<sup>55–57</sup> Jahan *et al.* have reported a tri-functional catalyst based on graphene oxide (GO)/Cu-MOF. It showed stability and catalytic activity towards ORR, OER, and HER.<sup>58</sup> The system had better charge transport and porosity due to synergy between Cu-MOF and GO. The GO/Cu-MOF offered a maximum power density of 110.5  $\text{mW cm}^{-2}$ , presenting itself as an economical alternative to Pt/C catalyst. MOF-based carbon nanotubes and graphene have also been studied several times owing to their high electrocatalytic efficiency.<sup>59,60</sup>

A recent study addressed this issue by introducing microperoxidase-11 (MP-11) into a recently discovered mesoporous MOF named as Tb-mesoMOF, thereby introducing novel MP-11@mesoMOF.<sup>61</sup> MP-11 with a heme center is a key player in peroxidase reactions and has been extensively used in biosensors, energy conversion, and biofuel cells. The application of MP-11 is limited due to its aggregation in solution, thus hindering accessibility of the heme group. The 3.0 and 4.1 nm pore size of Tb-mesoMOF easily accommodated MP-11 inside its nanoscopic framework, which was confirmed through decreased BET surface area from 1935  $\text{m}^2 \text{g}^{-1}$  to 400  $\text{m}^2 \text{g}^{-1}$ . Also, a color change from colorless to dark red was observed on saturation. A significant increase in the catalytic activity of MP-11@mesoMOF was observed as  $7.58 \times 10^{-5} \text{ mM s}^{-1}$  for approximately 30 min along with a higher substrate conversion of 48.7%. Furthermore, the recyclability of MP-11@Tb-mesoMOF is tested at different cycles. The MOF-enzyme system maintained its activity up to six cycles with no evidence of leaching due to strong hydrophobic interactions

between the MOF and enzyme, as shown in Fig. 6(a). This study is the first of its kind to use mesoporous MOF for enzyme immobilization and shows the tremendous potential of mesoporous MOFs as an ideal host matrix material for future use.

## 5.2 MOFs as electrolyte membranes

MOFs as electrolyte membranes is one of the largest research areas of MOF's applications in fuel cells. Exceptional super protonic conductivity as high as  $7.89 \times 10^{-2} \text{ S cm}^{-1}$  at 60 °C and 95% relative humidity (RH) with the help of MOF-808 has been achieved.<sup>62</sup> Conventionally, an ideal electrolyte membrane should be proton conducting, electrically insulating, and prevent fuel crossover. MOFs, despite their porous and crystalline structure, which contradicts proton-conducting membranes in fuel cells, emerged as one of the most promising electrolyte membranes due to several reasons.<sup>63</sup> A major reason being the presence of counter ions in MOFs, which favor proton conduction by both Grotthuss (proton hopping) and vehicle (self-diffusion) mechanisms.<sup>64</sup> Different counter ions containing hydroxyl, carboxylic, and ammonium-based functional groups have been used to functionalize MOFs for superior proton conduction through hydrogen bonding. Moreover, MOFs present an additional advantage through loading of suitable guest molecules in their pores in the prevention of fuel crossover and thus voltage loss.<sup>65</sup> It is also challenging to develop anhydrous proton conducting materials operational above 80 °C. To overcome this, imidazole has been encapsulated in aluminum MOF to form a hybridized polymer with superior proton conductivity in anhydrous conditions.<sup>66</sup>

Two MOFs with a common metal ion as aluminum but different organic linkers, namely NDC (1,4-naphthalenedicarboxylate) and BDC, were studied for proton conductivity with imidazole as a guest molecule. Imidazoles have an intermolecular proton transport pathway due to the two tautomeric forms alternating between two nitrogen atoms. Al( $\mu_2$ -OH)(ndc) showed a higher proton conductivity of  $2.2 \times 10^{-5} \text{ S cm}^{-1}$  that of Al( $\mu_2$ -OH)(bdc), which is  $1.0 \times 10^{-7} \text{ S cm}^{-1}$





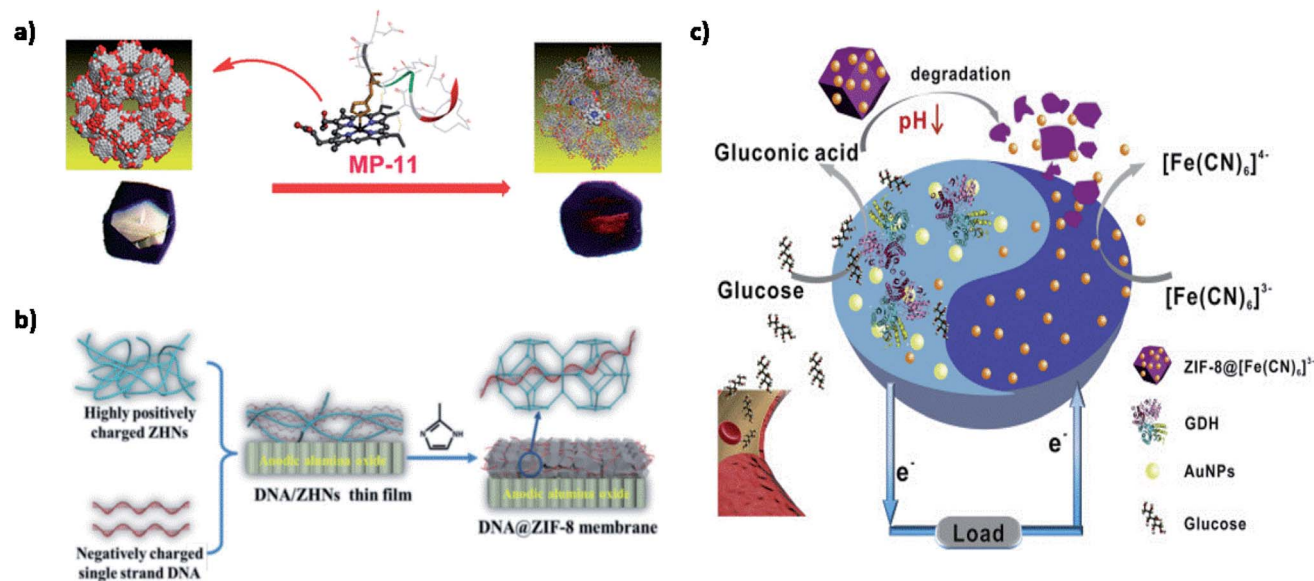


Fig. 6 Applications of MOFs in enzymatic biofuel cells. (a) MP-11@mesoMOF as an electrocatalyst.<sup>61</sup> (b) DNA@ZIF-8 as an electrolyte membrane.<sup>70</sup> (c) Anode-driven cathodic fuel release via pH-responsive ZIF-8 nanocarriers.<sup>82</sup>

at 120 °C. This can be explained by the hydrophobic pore surfaces of  $\text{Al}(\mu_2\text{-OH})(\text{bdc})$ , leading to increased host-guest interaction and hence decreased mobility. Similarly, histamine has been used as a guest molecule to achieve excellent proton conduction due to its unique structural behavior.<sup>67</sup>  $\text{Al}(\text{OH})(\text{ndc})$  encapsulated with histamine showcased proton conductivity of  $3.0 \times 10^{-3} \text{ S cm}^{-1}$ . This is due to intramolecular proton exchange in histamine facilitating reorientation, thereby increasing the rate of the Grotthuss mechanism. High concentration, approximately one histamine per aluminum ion, and its dense packaging in MOF contributed to increased proton conductivity. Better electrode kinetics and lower electrode poisoning can be achieved at higher temperatures but since many existing fuel cells rely on water for proton conduction, one major limiting factor in electrolyte membrane is their dehydration temperature. Based on Nafion, the gold standard of polymer electrolyte membrane, a sulfonated MOF called  $\text{Na}_3(\text{-thbts})$  ( $\text{thbts} = 2,4,6\text{-trihydroxy-1,3,5-benzene trisulfonate}$ ) was synthesized for potential anhydrous operation.<sup>63</sup> It was similar to Nafion, which is a sulfonated tetrafluoroethylene based fluoropolymer-copolymer having proton conductivity of  $2.0 \times 10^{-3} \text{ S cm}^{-1}$ . To make it operational at a high temperature of about 150 °C, water molecules in its structure were replaced with 1H-1,2,4-triazole (Tz) that achieved proton conduction in the range of  $2$  to  $5 \times 10^{-4} \text{ S cm}^{-1}$ .

Interestingly, the proton-conducting metal-organic framework 2 (PCMOF2) has been fabricated as a gas separator to prevent fuel crossover. Recently, a hybrid membrane of Zn-MOF/Nafion has been synthesized to improve the electrochemical performance of Nafion electrolyte membrane.<sup>68</sup> Better proton conductivity of  $7.29 \times 10^{-3} \text{ S cm}^{-1}$  has been achieved with 5% doping and 58% RH at 80 °C. The 1.87 times increase as compared to pristine Nafion membrane can be attributed to the host-guest hydrogen bonding, uncoordinated carboxyl

oxygen atoms, and sulfonic acid groups to enhance the acidity and hydrophilicity. Further,  $\text{NH}_3$  as a guest molecule was incorporated into this hybrid membrane to study its promotion effect. Zn-MOF- $\text{NH}_3$ /Nafion-5 exhibited nearly 5.47 times proton conductivity of the pristine Nafion membrane, which was  $2.13 \times 10^{-2} \text{ S cm}^{-1}$ . In addition to forming hydrogen bonds with the guest 1,2-bis(4-pyridyl)ethane molecule, Zn ions combined with intercalated water, resulting in the formation of different types of hydrogen bonds. Good single cell performance was recorded with a maximum power density of  $212 \text{ mW cm}^{-2}$  and a current density of  $630 \text{ mA cm}^{-2}$ , making it a promising high-performance Nafion hybrid membrane. Despite advancements in this field, the preparation of cost effective, non-toxic, and long-term structural stable electrolyte membranes is still a challenge.

Biocompatible MOFs are gaining interest due to their low toxicity, facile synthesis, and outstanding stability. Biomolecules/MOFs have been recently explored for their intrinsic proton conduction properties. Proteins and DNA found in the lipid bilayer are known to play an important role in proton and ion transmembrane transport. Inspired by this natural phenomenon, biomolecules have been used as proton carriers and proton donors for the successful generation of hydrogen bonds and coordination networks. Wang *et al.* have synthesized an amino acid-based Zr-MOF using L-aspartate spacer.<sup>69</sup> The MIP-202(Zr) had proton conductivity up to  $0.011 \text{ S cm}^{-1}$  at 363 K with 95% RH. This can be explained by accessible  $\text{NH}_3$  groups on aspartate linker acting as a proton source and mesoporous structure favoring hydrogen bond formation. The robust 3D microporous framework displayed good hydrolytic and chemical stability suitable for commercial production. Moreover, the tunable properties such as particle size and biocompatible linkers have opened up new avenues in the biotechnological and pharmaceutical industries. Similarly,



a DNA@ZIF-8 proton conducting membrane was developed by solid confinement conversion process.<sup>70</sup> The hydrophilic nature of DNA due to the presence of amidogen and phosphate groups improved the proton conductivity under 97% RH up to  $3.40 \times 10^{-4} \text{ S cm}^{-1}$  at 25 °C and  $0.17 \text{ S cm}^{-1}$  at 75 °C. Additionally, methanol crossover was significantly prevented due to a decrease in pore size upon loading of ssDNA (Fig. 6(b)). The system was successful in the construction of direct methanol fuel cells (DMFC) as MOFs-based PEM with a maximum power density of  $9.87 \text{ mW cm}^{-2}$ . Therefore, biomolecule modified MOFs as electrolyte membranes have encouraging results for improving electrochemical performance and stability. Besides this, the eco-friendly synthesis approaches should be explored for commercial outreach.

### 5.3 MOFs for fuel storage

Various porous materials like zeolites, ammonium phosphates, and coordination polymers have been extensively studied for application in fuel storage and transport. However, challenges in the development of robust synthesis methods and structurally stable porous networks over a wide range of temperature and pressure are still faced. Also, it is of key importance to maintain the interpenetrating network of porous materials that do not disintegrate upon the removal of guest molecules. MOFs present one such promising class of materials for the storage of fuels such as hydrogen, ethane, and methane with unique features of porous structure, high surface area, low density, and large-scale flexibility in comparison to the conventionally used zeolites<sup>71–73</sup>  $[\{[\text{CuSiF}_6(4,4\text{-bipyridine})_2] \cdot 8\text{H}_2\text{O}\}_n]$  was the first MOF to be reported as a novel methane adsorbent in 2000.<sup>74</sup> Based on argon adsorption, it had a specific surface area of  $1337 \text{ m}^2 \text{ g}^{-1}$ , micropore volume of  $0.56 \text{ mL g}^{-1}$  and was successful in similar adsorption capacity to that of zeolites and activated carbon.

MOFs have started to gain popularity as an ideal candidate for hydrogen storage in fuel cell technology due to their high energy density capability. The hydrogen uptake in MOFs largely depends on the heat of adsorption at low pressure, surface area at moderate pressure, and free volume at high pressure.<sup>75</sup> MOF-5 consisting of  $\text{Zn}_4\text{O}(\text{BDC})_3$  was the first to achieve reversible hydrogen adsorption up to 4.5 weight percent at 78 K, which is equivalent to 17.2 hydrogen molecules per formula unit.<sup>76</sup> At a pressure of 20 bar, 1.0 weight percent hydrogen adsorption at room temperature was observed, and increased loading capacity was found owing to two well defined hydrogen binding sites formed with zinc and the BDC linker. Similar experiments were replicated at room temperature and 10 bar pressure with IRMOF-6 and IRMOF-8, which interestingly gave doubled and quadrupled hydrogen uptake results, respectively, comparable to the highest capacity attained for carbon nanotubes at cryogenic temperatures.

There is a growing need to optimize hydrogen interactions, gravimetric (mass), and volumetric (size) surface area densities. It has been found that smaller pores in MOFs have higher hydrogen uptake capacity. In the case of large pores, the large voids may be reduced by interpenetration or catenation for

better efficiency. Strategies such as synthesis like topological modification in pore size,<sup>77</sup> framework catenation,<sup>78</sup> usage of additional adsorbate surfaces,<sup>79</sup> open metal sites,<sup>80</sup> and light metal MOFs<sup>81</sup> are being adopted to upscale the hydrogen affinity. Recently, ZIF-8 was explored for application in a smart membrane-less EBFC for the controlled release of cathodic fuel, as shown in Fig. 6(c).<sup>82</sup> The cathodic acceptor  $[\text{Fe}(\text{CN})_6]^{3-}$  was encapsulated within ZIF-8 to form  $[\text{Fe}(\text{CN})_6]^{3-}@\text{ZIF-8}$ , functioning as a pH responsive nanocarrier. ZIF-8 provided excellent pH sensitivity, stability and also decreased the internal resistance from the membrane. The LOD was recorded to be 1.6 mM with a maximum power density of  $23 \mu\text{W cm}^{-2}$ . The EBFC was driven by the production of gluconic acid up on glucose anodic oxidation.  $[\text{Fe}(\text{CN})_6]^{3-}@\text{ZIF-8}$  nanocarriers were degraded due to a change in pH to acidic, resulting in the regulated release of  $[\text{Fe}(\text{CN})_6]^{3-}$  into the electrolyte, thereby driving the electrochemical reaction between the anode and cathode. Further upgrades in the structure of the smart energy conversion devices could make a positive impact on the point-of-care technologies. Membrane-less systems are particularly attractive due to their low cost, high scalability, and superior power densities. However, care must be taken to ensure high reaction selectivity and maintain the optimum efficiency of bioelectrodes.

The porous structures can be utilized for advancements in fuel-cell powered vehicles and next generation clean energy storage. However, further studies are needed to balance between pore size and surface area of MOFs for maximum fuel storage at room temperature in fuel cells. Also, the complexity of synthetic modifications, poor stability, and narrow range of parameters limit the industrial applicability of MOFs.

## 6 Challenges and future prospects

MOFs have been explored extensively as promising materials for future EBFCs and self-powered biosensors. Researchers have concentrated their efforts to maximize the structural and functional advantages of MOFs into potential solutions for green energy production. Significant milestones regarding the use of MOFs and their derivatives in and as various components of EBFCs such as electrocatalyst, electrolyte membrane, biomolecule retention, and fuel storage have been achieved. MOF composites have shown tremendous potential in a variety of bioelectrochemical applications, as shown in Fig. 7. MOFs not only contribute to structural stability but also improve charge transfer and overall EBFC performance. MOFs established a strong foundation as substitutes for bioelectrode materials with superior biomolecule immobilization, fuel storage, and electrobiocatalysis to yield exceptional power output. The envisioned approaches are currently limited due to the high cost of commercially available MOFs. To address this, polyethylene terephthalate waste is hydrolyzed to obtain terephthalic acid for high value-added and cost-effective MOF synthesis. Few examples of MOFs such as UiO-66, MIL-101, and MOF-5 have already been synthesized through this approach.<sup>83</sup> It is noteworthy that MOFs can be used to deliver the utmost performance with facile synthesis. However, it is still



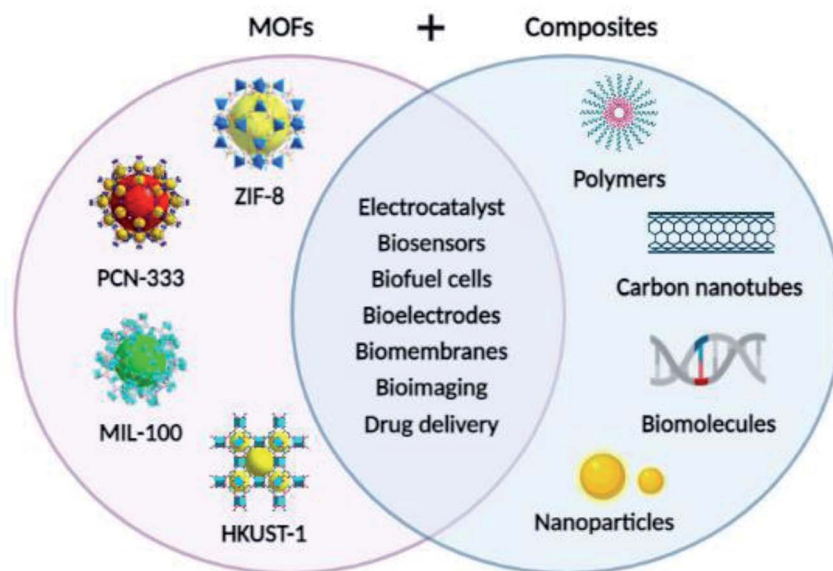


Fig. 7 Bioelectrochemical applications of MOFs and their composites.

a challenging task to carefully regulate their fine structure according to specific applications without affecting their advantageous properties. Advanced synthesis techniques are highly desirable in order to expand their industrial scalability by exploring MOFs with high hydrothermal stability. Post synthesis techniques such as solvent exchange and vacuum activation are commonly practiced that can be switched to less demanding and moderate condition requirements. In the case of characterization, the some techniques such as FTIR spectroscopy require the shaping of MOF powder into pellets, which can impact their surface texture and therefore, there is a need for further studies and improvements. From an application point of view, it is imperative to maintain the stability of MOFs in different solutions and prevent photodegradation. The behavior of MOF in water is an important parameter in defining their chemical stability.<sup>84</sup> For example, MIL-53 has been popular as an adsorbent due to its remarkable water stability.<sup>83</sup> With respect to the photostability of MOFs, it has been observed that terephthalate MOFs are more photostable than trimesate MOFs.<sup>86</sup> Recent development in the field of surface chemistry and nanobioelectronics have made significant contributions to expand MOF knowledge base. A better understanding of structure–property relation, enzyme–MOF interaction, and structural defects should be prioritized. More focus should be given to the application of MOFs in portable electronics for boosting their economic importance in the worldwide industry. More efforts are required for the translation of MOFs and MOF-based materials in implantable medical devices should be made.

## 7 Conclusions

Research and development of novel materials for bioelectrochemical applications have become a major thrust area in the energy sector. The pioneering work on MOFs catalyzed efficient energy conversion and storage, especially in EBFCs and

biosensors. MOF attracted a lot of attention in the fabrication of bioelectrodes for superior structure and function. Harnessing the inherent properties of MOF, such as high porosity, surface area, flexibility, and tenability, enables unique prospects in electrobiocatalysis, fuel storage, and biomolecule retention. In this review, MOFs have been highlighted as promising porous nanomaterials for application in EBFCs and biosensors. Various synthetic strategies, including post synthetic modification, have accelerated their applicability in diverse fields. Recent advances in MOF-based bioelectrodes to improve electrochemical performance and the long-term stability of EBFCs have been discussed. Remarkable outcomes have been achieved for the application of MOFs in and as host matrix to support biomolecule immobilization, synergistic biocatalyst to facilitate improved electron transfer, and BRE to increase the sensitivity and selectivity of bioelectrodes. This further enables more opportunities for the fabrication and miniaturization of energy devices. However, research on electroactive MOFs and their application are currently in the nascent phase. Despite encouraging theoretical results, it is of fundamental importance to achieve similar performance of MOF-based bioelectrodes in practical application. Also, the dynamic stability of MOFs in changing environments of pH and temperature for long durations is a prime concern. Efforts should be directed towards the facile and robust synthesis of bio-functionalized MOFs. MOF-based composite materials with high conductivity have been designed using metals as guest materials. These composites have surpassed the drawbacks of single component MOFs. However, poor cycle performance and conductivity of MOFs pose some challenges, which can perhaps be overcome by various techniques. Incorporation of ionic molecules or mobile counter ions within the MOF framework *via* post-synthetic modification can be used to boost the charge transport.<sup>87</sup> In-depth studies regarding host–guest interactions, biomimetic



MOFs and recyclability of these systems should be conducted for value-driven industrial scalability.

## Author contributions

Conceptualization – VA, SS and BDM, writing – original draft – VA and SS, writing – review & editing – BDM, supervision-BDM.

## Conflicts of interest

There are no conflicts of interest to declare.

## Acknowledgements

BDM acknowledges the DST – Science & Engineering Research Board (Government of India) for the award of Distinguished Fellowship (SB/DF/011/2019). SS is thankful to the CSIR India for the award of CSIR-RA fellowship. The authors thank the Vice Chancellor, Delhi Technological University, New Delhi for providing the opportunity to work in the lab.

## References

- 1 D. Shi, X. Yu, W. Fan, V. Wee and D. Zhao, *Coord. Chem. Rev.*, 2021, **437**, 213794.
- 2 H.-C. Zhou, J. R. Long and O. M. Yaghi, *Chem. Rev.*, 2012, **112**, 673–674.
- 3 G. Li and Y. Han, *ACS Cent. Sci.*, 2022, **8**, 150–152.
- 4 L. Jiao, J. Y. R. Seow, W. S. Skinner, Z. U. Wang and H.-L. Jiang, *Mater. Today*, 2019, **27**, 43–68.
- 5 H. Li, L. Li, R.-B. Lin, W. Zhou, Z. Zhang, S. Xiang and B. Chen, *EnergyChem*, 2019, **1**, 100006.
- 6 H.-F. Wang, L. Chen, H. Pang, S. Kaskel and Q. Xu, *Chem. Soc. Rev.*, 2020, **49**, 1414–1448.
- 7 S. Carrasco, *Biosensors*, 2018, **8**, 92.
- 8 C. Orellana-Tavra, R. J. Marshall, E. F. Baxter, I. A. Lázaro, A. Tao, A. K. Cheetham, R. S. Forgan and D. Fairen-Jimenez, *J. Mater. Chem. B*, 2016, **4**, 7697–7707.
- 9 H. Kaur, R. Kumar, A. Kumar, V. Krishnan and R. R. Koner, *Dalton Trans.*, 2019, **48**, 915–927.
- 10 L. Zhang, Z. Su, F. Jiang, L. Yang, J. Qian, Y. Zhou, W. Li and M. Hong, *Nanoscale*, 2014, **6**, 6590–6602.
- 11 C. Gong, Y. Shen, J. Chen, Y. Song, S. Chen, Y. Song and L. Wang, *Sens. Actuators, B*, 2017, **239**, 890–897.
- 12 A. Samui, A. R. Chowdhuri, T. K. Mahto and S. K. Sahu, *RSC Adv.*, 2016, **6**, 66385–66393.
- 13 G. de Combarieu, M. Morcrette, F. Millange, N. Guillou, J. Cabana, C. P. Grey, I. Margiolaki, G. Férey and J. M. Tarascon, *Chem. Mater.*, 2009, **21**, 1602–1611.
- 14 S. Maiti, A. Pramanik, U. Manju and S. Mahanty, *ACS Appl. Mater. Interfaces*, 2015, **7**, 16357–16363.
- 15 P. Sengodu, C. Bongu, M. Perumal and M. Paramasivam, *J. Alloys Compd.*, 2017, **714**, 603–609.
- 16 J. Yang, P. Xiong, C. Zheng, H. Qiu and M. Wei, *J. Mater. Chem. A*, 2014, **2**, 16640–16644.
- 17 N. Stock and S. Biswas, *Chem. Rev.*, 2011, **112**, 933–969.
- 18 F. Y. Yi, R. Zhang, H. Wang, L. F. Chen, L. Han, H. L. Jiang and Q. Xu, *Small Methods*, 2017, **1**, 1700187.
- 19 Y. Kobayashi, B. Jacobs, M. D. Allendorf and J. R. Long, *Chem. Mater.*, 2010, **22**, 4120–4122.
- 20 M. Kalaj and S. M. Cohen, *ACS Cent. Sci.*, 2020, **6**, 1046–1057.
- 21 C. H. Choi, S. H. Park and S. I. Woo, *ACS Nano*, 2012, **6**, 7084–7091.
- 22 S. Zhao, H. Yin, L. Du, L. He, K. Zhao, L. Chang, G. Yin, H. Zhao, S. Liu and Z. Tang, *ACS Nano*, 2014, **8**, 12660–12668.
- 23 A. E. Baumann, D. A. Burns, B. Liu and V. S. Thoi, *Commun. Chem.*, 2019, **2**(1), 1–14.
- 24 J. F. Olorunyomi, S. Teng Geh, R. A. Caruso and C. M. Doherty, *Mater. Horiz.*, 2021, **8**(9), 2387–2419.
- 25 M. G. Campbell, D. Sheberla, S. F. Liu, T. M. Swager and M. Dincă, *Angew. Chem.*, 2015, **127**, 4423–4426.
- 26 L. Sun, C. H. Hendon, M. A. Minier, A. Walsh and M. Dincă, *J. Am. Chem. Soc.*, 2015, **137**, 6164–6167.
- 27 T. C. Narayan, T. Miyakai, S. Seki and M. Dinca, *J. Am. Chem. Soc.*, 2012, **134**, 12932–12935.
- 28 C. Doonan, R. Riccò, K. Liang, D. Bradshaw and P. Falcaro, *Acc. Chem. Res.*, 2017, **50**, 1423–1432.
- 29 H. An, M. Li, J. Gao, Z. Zhang, S. Ma and Y. Chen, *Coord. Chem. Rev.*, 2019, **384**, 90–106.
- 30 W. Ma, Q. Jiang, P. Yu, L. Yang and L. Mao, *Anal. Chem.*, 2013, **85**, 7550–7557.
- 31 G. A. Udourioh, M. M. Solomon and E. I. Epelle, *Cell. Mol. Bioeng.*, 2021, **14**, 535–553.
- 32 P. Ling, J. Lei, L. Zhang and H. Ju, *Anal. Chem.*, 2015, **87**, 3957–3963.
- 33 P. Kumar, A. Deep, A. K. Paul and L. M. Bharadwaj, *J. Porous Mater.*, 2014, **21**, 99–104.
- 34 R. Ricco, P. Wied, B. Nidetzky, H. Amenitsch and P. Falcaro, *Chem. Commun.*, 2020, **56**, 5775–5778.
- 35 Y. Chen, V. Lykourinou, C. Vetromile, T. Hoang, L.-J. Ming, R. W. Larsen and S. Ma, *J. Am. Chem. Soc.*, 2012, **134**, 13188–13191.
- 36 G. Cheng, W. Li, L. Ha, X. Han, S. Hao, Y. Wan, Z. Wang, F. Dong, X. Zou, Y. Mao and S.-Y. Zheng, *J. Am. Chem. Soc.*, 2018, **140**, 7282–7291.
- 37 C. Wang, H. Sun, J. Luan, Q. Jiang, S. Tadepalli, J. J. Morrissey, E. D. Kharasch and S. Singamaneni, *Chem. Mater.*, 2018, **30**, 1291–1300.
- 38 Y. Zhang, F. Wang, E. Ju, Z. Liu, Z. Chen, J. Ren and X. Qu, *Adv. Funct. Mater.*, 2016, **26**, 6454–6461.
- 39 N. Jaiswal, C. M. Pandey, S. Solanki, I. Tiwari and B. D. Malhotra, *Microchim. Acta*, 2020, **187**, 1–8.
- 40 A. A. Ansari and B. D. Malhotra, *Coord. Chem. Rev.*, 2022, **452**, 214282.
- 41 X. Li, D. Li, Y. Zhang, P. Lv, Q. Feng and Q. Wei, *Nano Energy*, 2020, **68**, 104308.
- 42 X. Li, Q. Feng, K. Lu, J. Huang, Y. Zhang, Y. Hou, H. Qiao, D. Li and Q. Wei, *Biosens. Bioelectron.*, 2021, **171**, 112690.
- 43 W. Chen, W. Yang, Y. Lu, W. Zhu and X. Chen, *Anal. Methods*, 2017, **9**, 3213–3220.



- 44 X. Liu, W. Chen, M. Lian, X. Chen, Y. Lu and W. Yang, *J. Electroanal. Chem.*, 2019, **833**, 505–511.
- 45 C. Gu, L. Bai, L. Pu, P. Gai and F. Li, *Biosens. Bioelectron.*, 2021, **176**, 112907.
- 46 G. Yuan, L. Wang, D. Mao, F. Wang and J. Zhang, *Microchim. Acta*, 2017, **184**, 3121–3130.
- 47 M. Rasmussen, S. Abdellaoui and S. D. Minter, *Biosens. Bioelectron.*, 2016, **76**, 91–102.
- 48 S. Nara, R. Kandpal, V. Jaiswal, S. Augustine, S. Wahie, J. G. Sharma, R. Takeuchi, S. Takenaka and B. D. Malhotra, *Biosens. Bioelectron.*, 2020, **165**, 112323.
- 49 A. T. Yahiro, S. M. Lee and D. O. Kimble, *Biochim. Biophys. Acta, Spec. Sect. Biophys. Subj.*, 1964, **88**, 375–383.
- 50 M. Mon, R. Bruno, S. Sanz-Navarro, C. Negro, J. Ferrando-Soria, L. Bartella, L. Di Donna, M. Prejanò, T. Marino, A. Leyva-Pérez and D. Armentano, *Nat. Commun.*, 2020, **11**(1), 1–9.
- 51 C. Tudisco, G. Zolubas, B. Seoane, H. R. Zafarani, M. Kazemzad, J. Gascon, P. L. Hagedoorn and L. Rassaei, *RSC Adv.*, 2016, **6**, 108051–108055.
- 52 L. Zhang, X. Wang, R. Wang and M. Hong, *Chem. Mater.*, 2015, **27**, 7610–7618.
- 53 S. Dang, Q.-L. Zhu and Q. Xu, *Nat. Rev. Mater.*, 2017, **3**(1), 1–14.
- 54 B. Y. Xia, Y. Yan, N. Li, H. B. Wu, X. W. Lou and X. Wang, *Nat. Energy*, 2016, **1**(1), 1–8.
- 55 X. Wang, J. Zhou, H. Fu, W. Li, X. Fan, G. Xin, J. Zheng and X. Li, *J. Mater. Chem. A*, 2014, **2**, 14064–14070.
- 56 Y.-Z. Chen, C. Wang, Z.-Y. Wu, Y. Xiong, Q. Xu, S.-H. Yu and H.-L. Jiang, *Adv. Mater.*, 2015, **27**, 5010–5016.
- 57 J. Xi, Y. Xia, Y. Xu, J. Xiao and S. Wang, *Chem. Commun.*, 2015, **51**, 10479–10482.
- 58 M. Jahan, Z. Liu and K. P. Loh, *Adv. Funct. Mater.*, 2013, **23**, 5363–5372.
- 59 J. Wei, Y. Hu, Y. Liang, B. Kong, J. Zhang, J. Song, Q. Bao, G. P. Simon, S. P. Jiang and H. Wang, *Adv. Funct. Mater.*, 2015, **25**, 5768–5777.
- 60 L. Ge, Y. Yang, L. Wang, W. Zhou, R. De Marco, Z. Chen, J. Zou and Z. Zhu, *Carbon*, 2015, **82**, 417–424.
- 61 V. Lykourinou, Y. Chen, X.-S. Wang, L. Meng, T. Hoang, L.-J. Ming, R. L. Musselman and S. Ma, *J. Am. Chem. Soc.*, 2011, **133**, 10382–10385.
- 62 A. Sharma, J. Lim, S. Jeong, S. Won, J. Seong, S. Lee, Y. S. Kim, S. B. Baek and M. S. Lah, *Angew. Chem., Int. Ed.*, 2021, **60**, 14334–14338.
- 63 H. Kitagawa, *Nat. Chem.*, 2009, **1**, 689–690.
- 64 D.-W. Lim and H. Kitagawa, *Chem. Rev.*, 2020, **120**, 8416–8467.
- 65 J. A. Hurd, R. Vaidhyanathan, V. Thangadurai, C. I. Ratcliffe, I. L. Moudrakovski and G. K. H. Shimizu, *Nat. Chem.*, 2009, **1**, 705–710.
- 66 S. Bureekaew, S. Horike, M. Higuchi, M. Mizuno, T. Kawamura, D. Tanaka, N. Yanai and S. Kitagawa, *Nat. Mater.*, 2009, **8**, 831–836.
- 67 D. Umeyama, S. Horike, M. Inukai, Y. Hijikata and S. Kitagawa, *Angew. Chem., Int. Ed.*, 2011, **50**, 11706–11709.
- 68 H. Wang, Y. Zhao, Z. Shao, W. Xu, Q. Wu, X. Ding and H. Hou, *ACS Appl. Mater. Interfaces*, 2021, **13**, 7485–7497.
- 69 S. Wang, M. Wahiduzzaman, L. Davis, A. Tissot, W. Shepard, J. Marrot, C. Martineau-Corcus, D. Hamdane, G. Maurin, S. Devautour-Vinot and C. Serre, *Nat. Commun.*, 2018, **9**, 4937.
- 70 Y. Guo, Z. Jiang, W. Ying, L. Chen, Y. Liu, X. Wang, Z.-J. Jiang, B. Chen and X. Peng, *Adv. Mater.*, 2017, **30**, 1705155.
- 71 S. P. Shet, S. Shanmuga Priya, K. Sudhakar and M. Tahir, *Int. J. Hydrogen Energy*, 2021, **46**, 11782–11803.
- 72 U. Stoeck, I. Senkovska, V. Bon, S. Krause and S. Kaskel, *Chem. Commun.*, 2015, **51**, 1046–1049.
- 73 A. J. Pommer, S. Cal, A. H. Keeble, D. Walker, S. J. Evans, U. C. Kühlmann, A. Cooper, B. A. Connolly, A. M. Hemmings, G. R. Moore, R. James and C. Kleanthous, *J. Mol. Biol.*, 2001, **314**, 735–749.
- 74 S.-i. Noro, S. Kitagawa, M. Kondo and K. Seki, *Angew. Chem., Int. Ed.*, 2000, **39**, 2081–2084.
- 75 M. P. Suh, H. J. Park, T. K. Prasad and D.-W. Lim, *Chem. Rev.*, 2011, **112**, 782–835.
- 76 N. L. Rosi, J. Eckert, M. Eddaoudi, D. T. Vodak, J. Kim, M. O'Keeffe and O. M. Yaghi, *Science*, 2003, **300**, 1127–1129.
- 77 J. L. C. Rowsell and O. M. Yaghi, *Angew. Chem., Int. Ed.*, 2005, **44**, 4670–4679.
- 78 B. Chen, M. Eddaoudi, S. T. Hyde, M. O'Keeffe and O. M. Yaghi, *Science*, 2001, **291**, 1021–1023.
- 79 H. K. Chae, D. Y. Siberio-Pérez, J. Kim, Y. Go, M. Eddaoudi, A. J. Matzger, M. O'Keeffe and O. M. Yaghi, *Nature*, 2004, **427**, 523–527.
- 80 B. Chen, M. Eddaoudi, T. M. Reineke, J. W. Kampf, M. O'Keeffe and O. M. Yaghi, *J. Am. Chem. Soc.*, 2000, **122**, 11559–11560.
- 81 A. P. Côté and G. K. H. Shimizu, *Chem.-Eur. J.*, 2003, **9**, 5361–5370.
- 82 P. Gai, C. Gu, X. Kong and F. Li, *iScience*, 2020, **23**, 101133.
- 83 W. P. R. Deleu, I. Stassen, D. Jonckheere, R. Ameloot and D. E. De Vos, *J. Mater. Chem. A*, 2016, **4**, 9519–9525.
- 84 N. C. Burtch, H. Jasuja and K. S. Walton, *Chem. Rev.*, 2014, **114**, 10575–10612.
- 85 X. Qian, B. Yadian, R. Wu, Y. Long, K. Zhou, B. Zhu and Y. Huang, *Int. J. Hydrogen Energy*, 2013, **38**, 16710–16715.
- 86 N. K. Gupta, J. Bae, S. Kim and K. S. Kim, *RSC Adv.*, 2021, **11**, 8951–8962.
- 87 S. Kim, B. Joarder, J. A. Hurd, J. Zhang, K. W. Dawson, B. S. Gelfand, N. E. Wong and G. K. H. Shimizu, *J. Am. Chem. Soc.*, 2018, **140**, 1077–1082.
- 88 E. Zhang, Y. Xie, S. Ci, J. Jia and Z. Wen, *Biosens. Bioelectron.*, 2016, **81**, 46–53.
- 89 N. S. Lopa, M. M. Rahman, F. Ahmed, S. Chandra Sutradhar, T. Ryu and W. Kim, *Electrochim. Acta*, 2018, **274**, 49–56.
- 90 S. Zhou, L. Jiang, J. Zhang, P. Zhao, M. Yang, D. Huo, X. Luo, C. Shen and C. Hou, *Microchim. Acta*, 2021, **188**, 160.
- 91 Y. Song, M. Xu, C. Gong, Y. Shen, L. Wang, Y. Xie and L. Wang, *Sens. Actuators, B*, 2018, **257**, 792–799.





- 92 X. Wang, X. Lu, L. Wu and J. Chen, *Biosens. Bioelectron.*, 2015, **65**, 295–301.
- 93 H. Wang, Y. Jian, Q. Kong, H. Liu, F. Lan, L. Liang, S. Ge and J. Yu, *Sens. Actuators, B*, 2018, **257**, 561–569.
- 94 Y. Yu, C. Yu, Y. Niu, J. Chen, Y. Zhao, Y. Zhang, R. Gao and J. He, *Biosens. Bioelectron.*, 2018, **101**, 297–303.
- 95 T. Q. N. Tran, G. Das and H. H. Yoon, *Sens. Actuators, B*, 2017, **243**, 78–83.
- 96 F. Wang, X. Chen, L. Chen, J. Yang and Q. Wang, *Mater. Sci. Eng., C*, 2019, **96**, 41–50.
- 97 P. Zhang, H. Huang, N. Wang, H. Li, D. Shen and H. Ma, *Microchim. Acta*, 2017, **184**, 4037–4045.
- 98 C. Li, R. Wu, J. Zou, T. Zhang, S. Zhang, Z. Zhang, X. Hu, Y. Yan and X. Ling, *Biosens. Bioelectron.*, 2018, **116**, 81–88.
- 99 D. Arif, Z. Hussain, M. Sohail, M. A. Liaqat, M. A. Khan and T. Noor, *Front. Chem.*, 2020, **8**, 573510.
- 100 W. Meng, Y. Wen, L. Dai, Z. He and L. Wang, *Sens. Actuators, B*, 2018, **260**, 852–860.
- 101 Y. Yin, C. Gao, Q. Xiao, G. Lin, Z. Lin, Z. Cai and H. Yang, *ACS Appl. Mater. Interfaces*, 2016, **8**, 29052–29061.
- 102 Z. Kang, K. Jiao, R. Peng, Z. Hu and S. Jiao, *RSC Adv.*, 2017, **7**, 11872–11879.
- 103 F. Zhang, X. Wu, J. Gao, Y. Chen, Y. Gui, L. Zhang, W. Gan and Q. Yuan, *Electrochim. Acta*, 2020, **340**, 135958.
- 104 T. Yimamumaimaiti, X. Lu, J.-R. Zhang, L. Wang and J.-J. Zhu, *ACS Appl. Mater. Interfaces*, 2020, **12**, 41429–41436.
- 105 S. Cui, S. Gu, Y. Ding, J. Zhang, Z. Zhang and Z. Hu, *Talanta*, 2018, **178**, 788–795.
- 106 M. Rafti, W. A. Marmisollé and O. Azzaroni, *Adv. Mater. Interfaces*, 2016, **3**, 1600047.
- 107 S. Patra, S. Sene, C. Mousty, C. Serre, A. Chaussé, L. Legrand and N. Steunou, *ACS Appl. Mater. Interfaces*, 2016, **8**, 20012–20022.
- 108 J. Mao, L. Yang, P. Yu, X. Wei and L. Mao, *Electrochem. Comm.*, 2012, **19**, 29–31.

